International Journal of Engineering, Mathematical and Physical Sciences
ISSN: 2517-9934
Vol:1, No:6, 2007

Suspended Matter Model on Alsat-1 Image by MLP Network and Mathematical Morphology: Prototypes by K-Means

S. Loumi, H. Merrad, F. Alilat, and B. Sansal

***Abstract*—**In this article, we propose a methodology for the characterization of the suspended matter along Algiers's bay. An approach by multi layers perceptron (MLP) with training by back propagation of the gradient optimized by the algorithm of Levenberg Marquardt (LM) is used. The accent was put on the choice of the components of the base of training where a comparative study made for four methods: Random and three alternatives of classification by K-Means. The samples are taken from suspended matter image, obtained by analytical model based on polynomial regression by taking account of *in situ* measurements. The mask which selects the zone of interest (water in our case) was carried out by using a multi spectral classification by ISODATA algorithm. To improve the result of classification, a cleaning of this mask was carried out using the tools of mathematical morphology. The results of this study presented in the forms of curves, tables and of images show the founded good of our methodology.

***Keywords*—** Classification K-means, mathematical morphology, neural network MLP, remote sensing, suspended particulate matter

I. Introduction

THE oceans cover more than 70% of the surface of the Earth. They play a paramount role in the balance of the planetary ecosystem. The observation of the ocean from space allowed oceanographers to have on the one hand a global view of the phenomena observed and on the other hand to establish the relation between their temporal and spatial variability [1]. The color of the oceans is mainly due to the phenomena of the diffusion and absorption.

The sea water does not only consist of pure water, it also contains alive substances and various particles which modify its color. The variation of concentration of these various components determines the optical properties of the ocean. Consequently it modulates the radiation considered and acquired by sensors on board of the satellites [2].

In coastal and estuary zones, the mineral particles are comparable with the suspended materials. Often, only the properties of diffusion of this suspended particle matter (SPM) are considered and the properties of absorption are neglected. This approximation does not have a consequence in water of broad called water of the case 1 where the suspended materials are rare. But, in coastal water called water of case 2, the optical properties of water is much more complex to define because of diversity of the dissolved terrestrial contributions and materials in suspension.

The validation of the visible imagery and near infra-red in coastal water in general requires the description of empirical algorithms relating to a specific zone of study. Until the day of today, rare carried out work is developed based on empirical algorithms, valid for particular sites [3]. It is within this framework that our work is registered insofar as our objective is the characterization and the cartography of the suspended matter along the Algerian bay.

A significant fraction of the measurement observed by the satellite comes from the contribution of the atmosphere which overhangs the ocean. Marine reflectance accounts for only 10% of the total reflectance observed in blue and less still in the biggest wavelengths. It is thus essential to carry out a correction of the atmospheric effects. Georeferencing is also an essential step, it allows coinciding the positions of *in situ* measurements with the data images acquired by the sensors. These various treatments were carried out upstream of methodology [4].

In section 3 an image of the suspended particulate matter (SPM) is created by the establishment of a polynomial model. The Alsat-1 sensor bands used are those offering the best correlation between measurements in situ/bands values. In section 4, a particular care was taken to the creation of the mask where a method based on an unsupervised classification and the use of mathematical morphology, is proposed. The SPM image created is useful as bases training for neural network model (section 5). The results and the application are described in section 6.

Manuscript received December 17, 2005. Revised march 11 2006. This work was supported in part by l'ISMAL (Institut des Sciences de la Mer et de l'Aménagement du Littoral) and the University USTHB in the other part.

Saliha Loumi, Hamoud Merrad, Farid Alilat & Boualem Sansal are with University of Sciences and Technology Houari Boumediene. Faculté de Génie Electrique et d'Informatique. Institut d'Electronique, Laboratoire de Traitement d'Images et Rayonnement. BP 32, El-Alia Bab - Ezzouar, 16111, Alger Algérie. (Fax: +213 (21) 24-76-07 or +213 (21) 24-71-87, e-mail :salihaloumi@yahoo.fr, hmerrad@usthb.dz or merradhamoud@yahoo.fr , falilat@usthb.dz or falilat@yahoo.fr).

II. Site of Study and Sensor used

The region of interest is the bay of Algiers with geographical co-ordinates: 2°45 ' E with 3°45 ' E and 36°30 ' N with 36°60 ' N. The data used are multi spectral images acquired by the Algerian sensor Alsat-1 combined with *in situ* measurements.

The micro sensor Alsat-1[4] belonged to a new generation of micro sensor with great control capacity on altitude and orbit, and a high flow of remote loading. It is the first of a series of 05 micro sensors launched within the framework of the DMC (Disaster Monitoring Constellation) for the period going from 2002 to 2005. It launched on November 28, 2002 by the launcher Cosmos-3M starting from the Russian base of Plesetsk. The platform of the micro sensor has dimensions 60cm×60cm×60cm approximately in the configuration of launching. The communication is radio frequency type. The type SSDR of 9Gbits is used for memory storage. This memory can store images of an extent of 640kmx560km. The remote loading is carried out with a flow of 8Mbps.

The imagery system used is the ESIS (Extended Swath Imaging System), It rests on three spectral bands: (Green: 0.523 µm - 0.605µm), (Red: 0.629 µm - 0.690µm) and (Near Infra-red: 0.774 µm - 0.900µm), it uses the technology of imagery known as "pushbroom" with two cameras per band gone up in order to provide broad mown 600km and a space resolution of 32m. The standard size of a scene is 300km×300km, and is provided with two possible levels of processing:

- Level L0R: The three components (Near Infra-red, Red and Green) of the image are turned over vertically to be in conformity within the meaning of frame grabbing (direction trace of the satellite: ascending node). They are processed radiometricaly to correct on the one hand, the effects of vertical feature between the even and odd columns and on the other hand the effects of ornamentation with vignettes due to the optics camera.
- Level L1R: The three channels of level L0R are corrected for geometrical deformations due to the optics of each camera, and the orbital slope of the micro sensor.

III. Image of Reference of the Suspended Matter

In coastal water considering the space-time variability of its components, is difficult to model the suspended matter parameter [6][7]. We propose by our paper to characterize this parameter by the neural networks model. The number of in situ measurements being reduced, we propose to carry out an image of reference of the suspended matter using in situ measurements and establishing an analytical model which will be used as reference image for our network. The model carried out is by polynomial regression integrating in situ measurements and the radiometric values of spectral band at the points of measurements. The spectral bands used are those offering the greatest value of the correlation coefficient which analytical expression is given by (1)

$$R = \frac{\sum (X - \overline{X})(Y - \overline{Y})}{\sqrt{\sum (X - \overline{X})^2} \cdot \sqrt{\sum (Y - \overline{Y})^2}} \quad (1)$$

Where the vector Y represents in situ measurements of the suspended matter and $\overline{Y}$ its average, X is the standardized radiances of the various spectral bands at the point of measurements and $\overline{X}$ its average.

A. Polynomial Regression

It is a question of finding the best polynomial model as in (2) within the meaning of least squares passing by N points (x_i, y_i)

$$y = a_0 + a_1 x + \ldots + a_k x^k = \sum_{j=0}^{k} a_j x^j \quad (2)$$

The parameters a_j which minimizes the expression (3) are solution of (4)

$$E^2 = \sum_{i=1}^{N} e_i^2 = \sum_{i=1}^{N} [y_i - \sum_{j=0}^{k} a_j x_i^j]^2 \quad (3)$$

$$\sum_{i=1}^{N} \sum_{j=0}^{k} a_j x_i^{j+l} = \sum_{i=1}^{N} x_i^j y_i \quad l = 0,\ldots,k \quad (4)$$

The polynomial parameters are then given by (5)

$$a = (X^T.X)^{-1}.X^T.Y \quad (5)$$

B. Creation of the Mask

For the determination of the suspended matter, we propose a methodology, which imposes the creation of a mask allowing to consider only the water part of the image. This mask is carried out using a multi spectral classification. The method of classification used is unsupervised (no knowledge a priori). It is carried out with ISODATA algorithm. It consists in carrying out a partition of the multi spectral image (3 bands of the Alsat-1 image) in two classes (water/land). Zero value (0) is allotted to the land whereas the value one (1) is allotted to water.

To improve the result of this classification, a cleaning of the mask is necessary (Fig. 1). We thus called upon the tools of mathematical morphology.

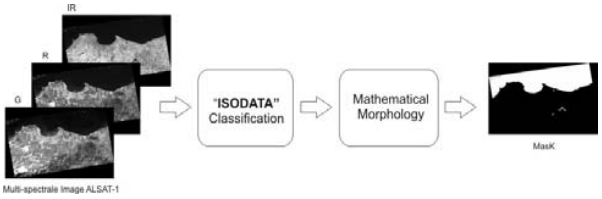

Fig. 1 Diagram block of the determination of the mask

VI. Mathematical Morphology

Mathematical morphology [8][9] considers that the distribution of the values in the image forms objects. The

morphological operations consist in transforming sets by the action of a structuring element B modifying the set by union, intersection or complementation. The choice of the structuring element depends on the type of required information.

A. Opening and Closing

We call open X by B, unit X_B formed by the union of all the elements B included in X as (6)

$$X_B = \bigcup_{b \in B} \left(\bigcap_{b \in B} X_{ob} \right) \tag{6}$$

While referring to the elementary operations of erosion and dilation X_B is practically obtained by an erosion of X by B followed by the dilation of the result by B as follows in (7)

$$\begin{aligned} & X_B = (X \Theta B) \oplus B \\ \text{with} \quad & X \Theta B = \left\{ x / B_x \subset X \right\} \\ \text{and} \quad & X \oplus B = \left\{ x / B_x \cap X \neq \phi \right\} \end{aligned} \tag{7}$$

Closing X^B is a dual operation of the opening; it is defined by (8)

$$\begin{aligned} X^B = ((X^c)_B)^c &= ((X^c \Theta B) \oplus B)^c \\ &= (X \oplus B) \Theta B \end{aligned} \tag{8}$$

B. Conditional Dilation

The successive dilations applied only inside unspecified part or the starting whole of another unit constitute the operation of conditional dilation. Either M parts of unit X; the dilation of M in X by B is expressed by (9)

$$Y_1 = (M \oplus B) \cap X \tag{9}$$

If this operation is reiterated N time we will have (10)

$$Y_n = \underbrace{(\ldots((M \oplus B) \cap X) \oplus B \cap X) \ldots \cap X) \oplus B \cap X}_{n\,time} \tag{10}$$

This continuation is convergent and stops when Yn-1 = Yn. This operation represents the invasion of a particle of a unit since a marker M until idempotence.

V. Multi Layer Perceptron Model (MLP)

We propose a multi layers perceptron (MLP) as model for the determination of the concentration of the suspended matter [10]. The network model has a layer of input, a hidden layer and an output layer having 3, 5 and 1 neurons respectively. The training of the network is done by back propagation of the gradient optimized by the algorithm of Levenberg Marquardt (LM) [11]. The result image obtained is multiplied by the mask previously given (Fig. 2).

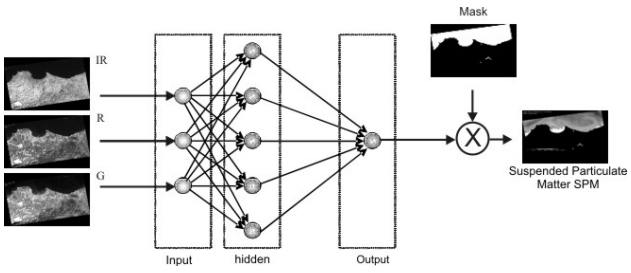

Fig. 2 Modeling of SPM by MLP

In the multi layers perceptron (MLP) with training by retro propagation of gradient [12], the gradient gives the direction towards which it is necessary to move to find the minimum of the error, but does not give the step with which one must modify the weights of the network to make decrease as fast as possible this error [13], indeed this step is a fixed or adaptive coefficient (variable for each iteration). The algorithm of Levenberg-Marquardt [13] [14] [15] makes it possible to determine this step by using the derivative second expression of the average quadratic error. This quadratic error is expressed by (11)

$$F(w) = \left\langle (g(a,w) - b)^2 \right\rangle \tag{11}$$

where $\langle\ \rangle$ is the average calculated on the whole couples (a, b) and g is a function of two vectors a and w. The idea consists of the determination of the new weight vector wt_{+1} according to current w_t, such as the value of F (wt_{+1}) approaches more than one local minimum of the function F. For that, we calculate a quadratic approximation of F starting from a linear approximation of g around the point w_t.

By determining the point w_t for which the gradient of the quadratic approximation of F is cancelled, we obtain (13) and (14)

$$w = w_t - H^{-1} d \tag{12}$$

with

$$d = \left\langle (g(a,w_t) - b)\ \nabla g(a,w_t) \right\rangle \tag{13}$$

$$H = \left\langle \nabla g(a,w_t)\ \nabla g(a,w_t)^T \right\rangle \tag{14}$$

Equation (12) could be used in the determination of wt+1 starting from wt for the condition that g is close to a line around wt. The use of this quadratic approach in the area where g is quasi linear is a descent of the gradient, in the contrary case it represents the concept of Levenberg - Marquardt. Formulation is given by (16).

$$w_{t+1} = w_t - (H + \lambda I)^{-1} d \tag{15}$$

Indeed, when λ has a small value, (15) is equivalent to (12), and if λ is large it is equivalent to (16)

$$w_{t+1} = w_t - \frac{1}{\lambda} d = w_t - \frac{1}{2\lambda} \nabla F(a, w_t) \tag{16}$$

Equation (16) is a descent of the gradient. In practice we proceed as (17)

$$F(w) = \sum_{p=1}^{P}\sum_{k=1}^{K}(d_{kp} - o_{kp})^2 \quad (17)$$

where $w = [w_1 w_2 \ldots\ldots w_N]^T$ is the weight vector of the network between the two layers considered, d_{kp} is the desired value of the node k of the output layer for the example p, o_{kp} is the current value obtained by the network with the node K for the example p; P is the number of examples, and K the number of nodes of the output layer. Equation (11) can be written according to the vector of cumulative error E as (18)

$$F(w) = E^T E \quad (18)$$

$E = [e_{11} \ldots e_{K1} e_{12} \ldots e_{K2} \ldots\ldots e_{1P} \ldots e_{KP}]^T$, $e_{pk} = d_{pk} - o_{pk}$, k = 1,…, K and p = 1, …, P.

The updated weights are as (19)

$$w_{t+1} = w_t - \left(J_t^T J_t + \lambda I_t\right)^{-1} J_t^T E_t \quad (19)$$

where J is the Jacobian matrix, w_{t+1} and w_t are the new and old weight respectively. I is the matrix identity and λ a fixed constant parameter. It is obvious that this process is particularly interesting to make converge the neural network in a less iteration count, but it is clearly also that each iteration requires more computing because of inversion of the matrix.

A. Creation of the Training Base

The base of training of such neural network strongly influences the quality of the result. An optimal choice has a primary importance. This choice strongly depending on the number and the distribution of the samples, two steps was considered and compared

• Selection in a random way of the samples.

• Unsupervised multi spectral classification of the all samples in K classes of the whole samples corresponding to the water part. In phase of training, we have fixed the average quadratic error to reach at 10^{-7}. In phase of generalization, the comparison criterion is the root mean square error (RMS) which has expressed by (20)

$$RMS = \sqrt{\frac{1}{N}\sum_{i=1}^{N}(Yréf - Yest)^2} \quad (20)$$

Where Yref and Yest are the reference and estimated images of SPM. N is the point's numbers of the image reference.

For the first step, we carry out a selection of a K number of samples among the whole of the samples corresponding to the water part and their correspondents in the SPM image of reference. It is obvious, by this manner of proceeding, that no control on the spectral distribution of the samples of this base is possible, and that only the control of the number can be it.

B. Classification by the K-Means

The base of training is made up after not supervised multi spectral classification of all the samples in K classes by using the algorithm of the K-Means of the pixels of the water part. We will have to consider the K nearest samples to the barycentre of K classes. The co-ordinates in row and column of each representative class will indicate SPM in the image of reference (Fig. 3).

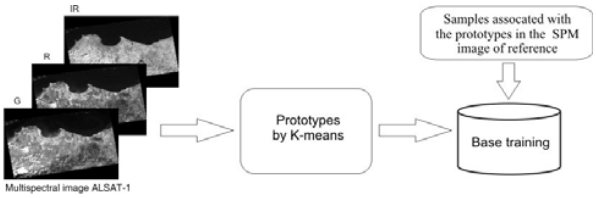

Fig. 3 Determining of training base

Algorithm:

Step 1: Choose K center class arbitrarily

Step 2: Distribute all the points P on these K classes, according to the rule:

$$P \to Sj \text{ If } \forall\ i \neq j\ \ \|P - mj\| \leq \|P - mi\|$$

P: Pixel of the image; mi , mj , Averages of the classes Si and Sj .

Step 3: Calculate the new center class,

$$mj = \frac{1}{Nj}\sum_{x \in Sj} P \text{ ,} \quad \text{Nj: samples of the class J}$$

Step 4: If the center class moved, return to step 2 if not end.

Step 5: Take in each class the element nearest to the barycentre.

Three alternatives of the technique were considered:

• With redundancy: all the water pixels are considered. It is clear that the same pixel will be in its class as many once as it to appear in the image. The barycentre of this class will be strongly influenced.

• Without redundancy: the same pixel is considered only once in classification.

• Without redundancy but with substitution of the identical samples. This substitution will be done after classification while not taking (as far as possible) as representatives of classes only those which have the different SPM ones.

VI. Results and Application

With our data the highest correlation is given in Table 1 by the spectral band (0.523 µm - 0.605µm). This band was used for the polynomial regression and the obtained model is given by (21).

$$\hat{y} = -635.3 + 2.57x - 0.1197x^2 \quad (21)$$

TABLE I
CORRELATION COEFFICIENT FOR *IN SITU* MEASUREMENTS AND ALSAT-1 IMAGE

Band (μm)	0.523- 0.605	0.629-0.69	0.774 - 0.90
R^2	0.9049	0.8016	0.5486

Classification by ISODATA (Fig.4a) gives a rather good separation between the sea and the land (almost smooth line of coast) to the detriment of some imperfections. The opening by a disc B of 17 pixels diameter allowed us to clean the mouth of oued (river) El Harrach (Fig.4b and Fig.4c). The imperfections of the bottom left (Fig.4d) were eliminated by a closing with a segment having 100 pixels and a direction of 8.5° compared to the horizontal (Fig.4e). The conditional dilation associated to the four markers (sea, and three bridges Keddara, El-Hamiz and Réghaïa) allowed us to eliminates all undesirable asperities (Fig.4f).

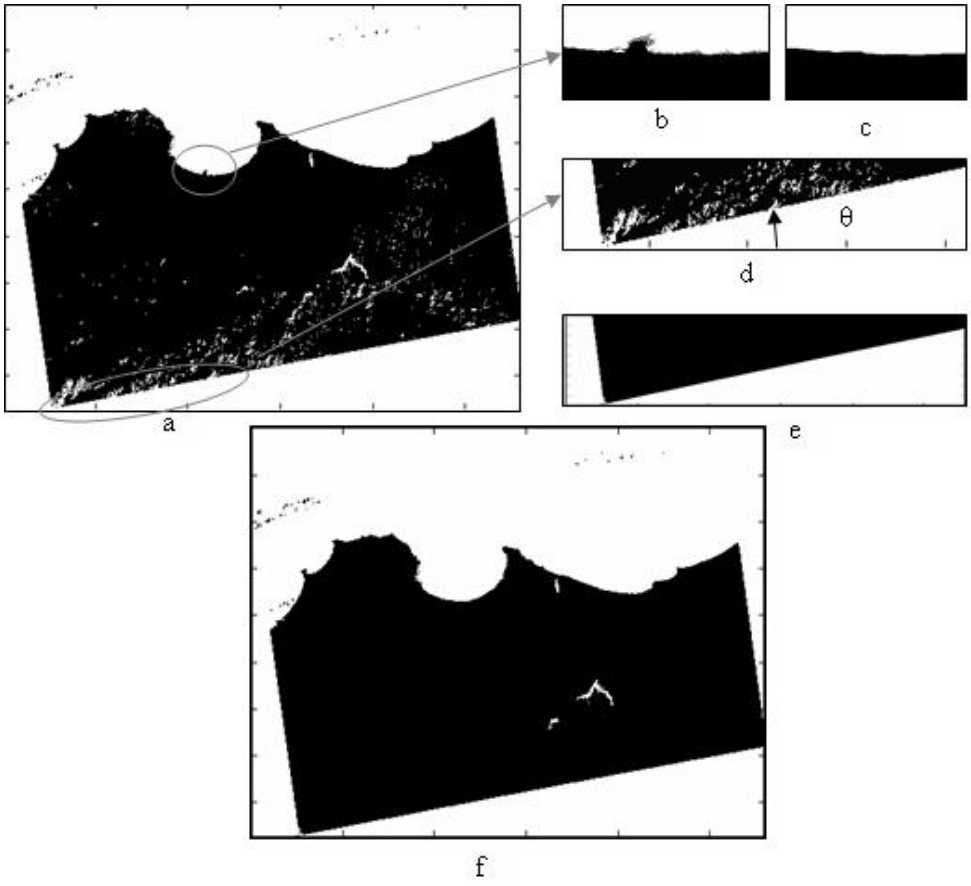

Fig. 4 Cleaning of the mask obtained by classification ISODATA of the Alsat-1 image

For the choice of the training base, a study according to the size of the base emphasizes (Table 2) that 100 samples taken in a random way give a result better than that of 500 samples and the best precision is obtained for 800 samples. The evolution of the error seems in contradiction with work affirming that more the number of samples is high, better is the training thus the precision. We sought for each case, the number of effective samples (those which do not have the same value of SPM) (Table 2). It is clear that the weakest error of generalization was obtained for 800 samples, and that this corresponds to a number of effective highest samples (37).

TABLE II
INFLUENCE SIZE OF THE BASE IN THE RANDOM CASE

Samples	100	300	500	700	800	900	1000
RMS	0.934	1.333	1.315	0.480	0.468	0.507	0.556
Effective samples	22	30	29	31	37	37	34

As for the choice of the prototypes by the second alternative, the study was done for seven (07) bases of sizes: 10, 30, 50, 70, 80, 90 and 100 samples. Each element of a base corresponds to a representative of a class. The number of effective samples for each alternative is given by table 3.

TABLE III
EFFECTIVE SAMPLES FOR THE THREE ALTERNATIVES

Samples / Effective samples	10	30	50	70	80	90	100
With redondancy	9	16	21	17	24	23	26
With out redondancy	8	23	29	33	32	32	36
With out redondancy and substitution	10	30	49	46	50	50	50

According to curves of the root mean square error in generalization (Fig. 4), we note that classification without redundancy and substitution gives a better precision for a number of samples between 15 and 35. Beyond 65 samples, the best results were given by classification without redundancy. This error RMS varies very little beyond 80 samples. This result not being foreseeable, we then tried to find an explanation, by considering the two particular bases: 30 and 90 samples. For these two cases, the performances of the two steps quoted previously are reversed compared to the third alternative (classification with redundancy) (Fig. 5).

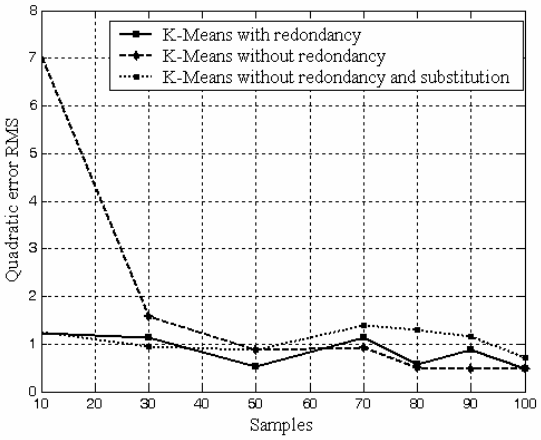

Fig. 5 Influence of samples to the quadratic error for three alternatives

These results are explained by the frequency of appearance of SPM in the base of training (Fig. 6) where the best result is justified by the spreading out of dynamics.

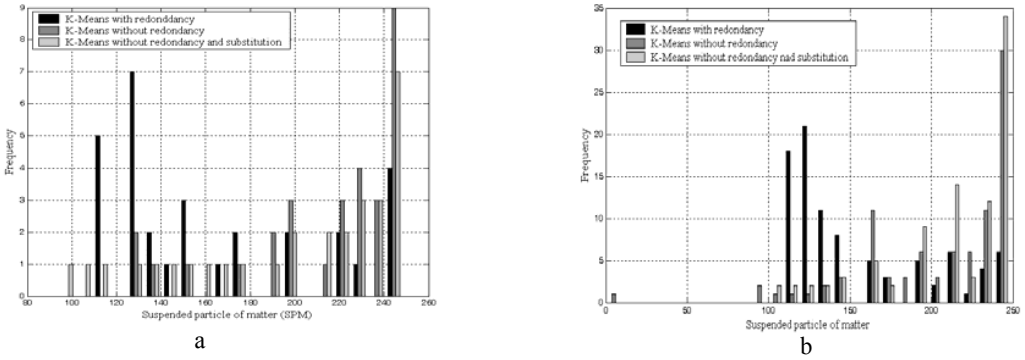

Fig. 6 Dynamics of the samples of the bases for (a) 30 and (b) 90 samples

We tested our methodology in a field of particular interest, and which lies within the scope of the natural disasters such as the floods and the seism, to explain certain direct or indirect consequences on coastal water. We used an image of the 24/5/2003 (03 days after the earth quake which struck the area of Boumerdès which is locate at 40km in the east of Algiers), acquired by the Alsat-1 sensor and which covers the zone touched by the seism. We cut out this rough image a scene of size 600x2400 pixels which we corrected and georeferenced.

We then applied the neural model determined previously to obtain the image of the suspended matter. The result image of generalization (figure 7) reveals us a zone of strong suspended matter concentration localised close to the epicentre (white color). This can be justified by the fact that under the effect of the jolt and the repeated counterparts, an agitation of sea-beds caused an increase of the suspended matter towards the surface of the sea.

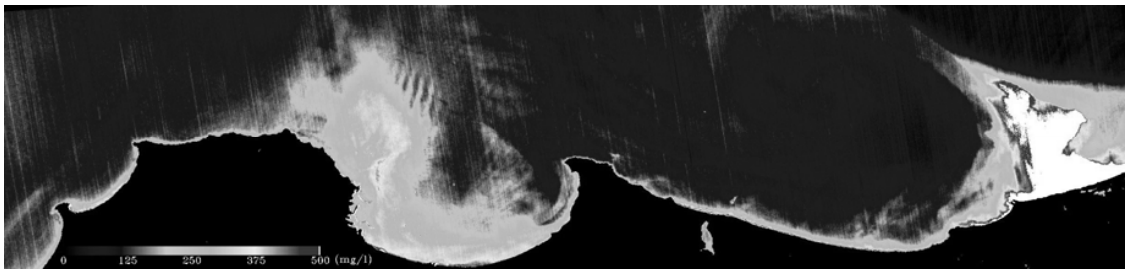

Fig. 7 Result image SPM at the 24/05/2003

VII. CONCLUSION

This study is the first results of a methodology in which we combined multi spectral images of the ALSAT-1 sensor and *in situ* measurements for a characterization of the suspended particulate matter (SPM) along the Algerian coast. A model by the multilayer perceptrons (MLP) was implemented. An architecture corresponding to three (03) input cells, a hidden layer of five (05) cells and an output with a one cell was adopted. In this step, the accent was laid on the choice of the prototypes of the training base where a comparative study was made for four different methods: a random selection of the samples and three alternatives of the selection by K-Means classification. Through this study, it appeared that for the constitution of the training base, two significant elements are to be taken into account:

- Richness of the base which is expressed by the number of samples.
- The representativeness of the base which depends on the distribution of these samples.

A better representativeness is obtained when the samples occupy all the dynamics of the possible values. A particular care was to bring to the creation of the mask, where an unsupervised classification by ISODATA and cleaning by the quite selected tools of mathematical morphology gave full satisfaction. By the method suggested we could on the one hand improved the performances of the network by carrying out a good compromise between a number of samples and representativeness of the base and on the other hand highlighted the phenomenon of the increase of the suspended matter towards surface of the sea, had with the agitation of the sea-beds, caused by the repeated jolt and counterparts which touched the area of Boumerdes on May 21, 2003.

ACKNOWLEDGMENT

The authors wish to thank the ASAL (Algerian Agency Space) Institute for the Alsat-1 images, and the ISMAL institute (Institute of Marine Science of the Algerian Littoral) for *in situ* measurements.

REFERENCES

[1] D. K Hall., J. R. Key, Casey K. A., G. A. Riggs , D. J. Cavalieri., " Sea Ice Surface Temperature Product from MODIS," *IEEE Trans. Geoscience Remote Sensing*, , 2004, vol. 42, no. 5, May pp. 1076-1087.

[2] L. Parkinson, "Aqua: An Earth-Observing Satellite Mission to Examine Water and Other Climate Variables," *IEEE Trans Geoscience Remote Sensing*, 2003, vol. 41, no. 2, Feb pp. 173–183.

[3] J. M Froidefond , D. Doxaran, " Télédétection Optique Appliquée à l'étude de eaux côtières," *Télédétection*, 2004, vol. 4, no. 2, pp. 157-174.

[4] H. Merrad, "Caractérisation des Eaux Côtières à partir d'Images Multi spectrales de MODIS et ALSAT-1 : Application au littoral Algérien, " Thèse de Magister, 2005, Université des Sciences et de la Technologie Houari Boumediene à Alger,.

[5] M. Bekhti, A. Oussedik, J.R. Cooksley. " Alsat-1: Conception details and in orbit performance, " *Actes des Journées Techniques ALSAT 1/ Utilisateurs,* 2003, Juillet 14 et 15 , Alger.

[6] D.B. Patissier, G.H. Tilstone, V.M. Vincente & G.F. Moore, "Comparaison of bio-physical marine products from SeaWiFs, MODIS and a bio-optical model with in situ measurements from Northern European waters," .2004, *Journal of Opitcs,* pp. 875-889.

[7] D. Doxaran, J. M. Froidefond, S Lavender & P. Castaing, "Spectral signature of highly turbid waters Application with SPOT data to quantify suspended particulate matter," *Remote Sensing of Environment*, 2002,81, 149-161,

[8] M.Coster ET J. L.Cherman, "Précis d'analyse d'images," 1985, *Éditions du CNRS*.

[9]] J. Serra. "Image Analysis and Mathematical Morphology," 1982 *Academic Press, London*.S.

[10] Haykin, "Neural Networks: A Comprehensive Foundation," 1999 *Second edition, Prentice Hall*.

[11] F. Alilat, S. Loumi, H. Merrad & B. Sansal, "Nouvelle approche du réseau ARTMAP Flou Application à la classification multispectrale des images SPOT XS de la baie d'Alger," *Revue Française de Photogramétrie et de Télédétection SFPT*, (2005-1),.no.177, pp 17-24.

[12] Z. Zhou, Chen & Z. Chen, "FANNC*:* A Fast Adaptive Neural Network classifier," 2000*, Knowledge and Information Systems*, Vol. 2, N°1, pp. 115-129.

[13] P. Baldi, "Gradient Descent Learning Algorithm Overview: A General Dynamical Systems Perspective," 1995*, IEEE Transactions on Neural Networks*, Vol. 6.

[14] M. Hagan T. & M .B. Menhaj, "Training Feed forward Networks with the Marquardt Algorithm,", 1994, *IEEE Transactions on Neural Networks*, Vol.5 No 6.

[15] B.M. Wilamowskin, S. Iplikci, O. Kaynak & Efe, "An Algorithm for fast Convergence in Training Neural Networks," 2001, IJCNN'01, Washington C. c July 15-19 , pp. 1778-1782.

Saliha Loumi has received her diploma in electronics engineer from polytechnic school Algiers in 1983, and magister diploma in electronics in November 14, 1889. She is currently completing theses of state doctorate at the University of Sciences and technology Houari Boumediene (USTHB).
She is lecturer and charged of research 1992 à USTHB University. She has done research in pattern recognition, multi-image processing, remote sensing, texture analysis and data compression.
Her present research interests lie in applied mathematical morphology, image processing.

Farid Alilat has received his diploma in electronics engineer at the University of Sciences and technology Houari Boumediene (USTHB) in 1988, and magister diploma in electronics in June 1992, Algeria. He is currently completing theses of state doctorate.
He is charged of research and lecturer at this university (USTHB) since 1993. He has done research in classification, pattern recognition, clustering, remote sensing, and data compression, artificial intelligence.
His present research interests lie in applied mathematics, image processing and neural networks. Actually, F. Alilat is a reviewer for the International Journal of Remote Sensing (IJRS).

Hamoud Merrad received his diploma in electronic engineer from the National Polytechnic school of Algeria in February 1986 and magister diploma in electronics in November 2005.
He is currently a researcher and a lecturer at the University of Sciences and technology Houari Boumediene (USTHB).
His research interests include remote sensing, methodologies for the determination of atmospheric and marine properties.

Sansal Boualem has received her professor diploma in electronics engineer from the university of England.
In 1980, he has worked for the Nuclear Center of Research, in Algeria and in 1989 he joined the faculty of department of electronic and informatics of USTHB University.
Prof. Sansal is responsible for development of GIP (Group Image Processing) and, a director of Image processing and radiation laboratory of Algeria University.